Steady state heat transfer in microcracked media

Sharan Raj RANGASAMY MAHENDREN, Hélène WELEMANE*, Olivier DALVERNY, Amèvi TONGNE

Université de Toulouse; INP/ENIT; LGP; 47 Avenue d'Azereix, F-65016, Tarbes, France + helene.welemane@enit.fr

Abstract:

Material behaviour is often affected by the heterogeneities existing at the microscopic level. Especially the presence of cracks, voids, etc collectively known as defects, can play a major role in their overall response. Homogenization can be used to study the influence of these heterogeneities and also to estimate the effective properties of a given material. Several research works have been dedicated to determine the elastic behaviour of a microcracked media. Yet, thermal properties are not investigated as much. Moreover, the question of unilateral effect (opening/closing of cracks) still remains an important issue. So, this paper aims to provide the effective thermal conductivity of a microcracked media with arbitrarily orientated cracks, either open or closed. With the help of Eshelby-like approach, homogenization schemes (dilute and Mori-Tanaka) are developed to provide the closed-form expression. In addition, numerical simulations based on Finite Element Modelling are also performed to validate and analyze the obtained results.

Keywords: Homogenization / heat conduction / microcracking / unilateral effect / simulations

1 Introduction

Defects have an influence on the macroscopic behaviour of a material, each on a different scale. The overall behaviour of the material can be characterized by its microstructure. This transition from micro-to-macro can be modelled using averaging techniques (homogenization). In this process, the heterogeneous material is replaced by an equivalent continuous medium. By this way, one can find the effective properties of a material. Homogenization studies often concentrate only on the mechanical behaviour of a microcracked material [1, 2], leaving out thermal and other properties. But the latter have practical applications too and need to be investigated [3, 4].

Apart from the orientation of the cracks, opening or closing of microcrack (also known as unilateral effect) can have a different influence on the material, in turn on the overall properties. Consequences of both induced anisotropy and unilateral effect on the elastic problem have been studied by some authors [1, 5] but not much for the heat conduction problems. We intend here to propose an Eshelby-like modelling approach for the steady state heat transfer and determine the effective thermal conductivity. We also intend to provide some numerical results in order to validate and analyze the theoretical results.

2 Theoretical Framework

Current works on the effective thermal properties are influenced by the similarities between elasticity and steady-state heat conduction variables [6]. Similar to the macroscopic stress and strain under equilibrium conditions, the macroscopic heat flux Q and temperature gradient G corresponds to the average values of their respective microscopic quantities q and g under stationary thermal conditions i.e. $G = \langle g \rangle$ and $Q = \langle q \rangle$. The linear thermal behaviour is given by the Fourier law:

$$q = -\boldsymbol{\lambda} \cdot g \tag{1}$$

where $\boldsymbol{\lambda}$ is the symmetric second order thermal conductivity tensor.
Let us consider a 3D RVE of a microcracked media. Such media exhibits a matrix-inclusion topology in which each phase exhibits a homogeneous behaviour. A uniform macroscopic temperature gradient G is imposed at the outer boundary $\delta\Omega$ of the RVE . Assuming an initial natural state, the microscopic and macroscopic quantities can be linked linearly as [7]:

$$g(x) = \mathbf{A}(x) \cdot G \qquad \forall\, x \in \Omega \tag{2}$$

where $\mathbf{A}$ is the second order temperature gradient localization tensor. Similar to (1), the overall behaviour of the RVE can be given by:

$$Q = -\boldsymbol{\lambda}_{hom} \cdot G \tag{3}$$

where $\boldsymbol{\lambda}_{hom}$ is the overall thermal conductivity of the microcracked media. Assuming the condition $\langle \mathbf{A} \rangle = \mathbf{I}$ and (2), the effective thermal conductivity of the microcracked media is given by:

$$\boldsymbol{\lambda}_{hom} = \boldsymbol{\lambda}_m + f_c \left(\boldsymbol{\lambda}_c - \boldsymbol{\lambda}_m\right) \cdot \langle \mathbf{A} \rangle_c \tag{4}$$

where $\boldsymbol{\lambda}_m$ (resp. $\boldsymbol{\lambda}_c$) is the conductivity tensor of the matrix (resp. cracks), f_c is the cracks volume fraction and $\langle \cdot \rangle_r = \frac{1}{\Omega_r} \int_{\Omega_r} \cdot \, d\Omega$ denotes the mean value over the volume of the phase r for $r = \{m, c\}$.
The single-inhomogeneity problem studied by Eshelby [8] considers a single ellipsoidal inclusion embedded inside an infinite matrix subjected to macroscopic stress or strain tensors at infinity. This elasticity problem can be extended to thermoelasticity [6, 9]. In such case, the local temperature gradient in the crack can be approximated by the uniform local field obtained for an ellipsoid embedded in an infinite matrix subjected to uniform boundary condition G_∞.
For our case, let us consider an RVE composed of an initially isotropic homogeneous media (matrix). Its thermal conductivity tensor is given by $\boldsymbol{\lambda}_m = \lambda_m\, \mathbf{I}$ (λ_m is the matrix scalar thermal conductivity). This matrix is weakened by randomly distributed single family of parallel microcracks (Fig. 1-a). These cracks are modelled as flat oblate ellipsoid (mean semi-axes a

and c, Fig. 1-b) with a volume fraction f_c=$\frac{4}{3}\pi d\omega$. Here $d = \mathcal{N}a^3$ is the scalar crack density as defined by Budiansky and O'Connell [10] and $\omega = {}^{c}\!/_{a}$ is their mean aspect ratio. Taking all this into account and considering $\mathbf{n}$ as the unit vector normal to the crack plane, estimated solutions for localization tensor over the crack's phase $\langle \mathbf{A} \rangle_c$ can be determined. They depend on the following depolarization tensor $\mathbf{S}_E$ (similar to the Eshelby tensor of the elastic problem) [11]:

$$\mathbf{S}_E = \left(1 - \frac{\pi}{2}\omega\right) \mathbf{n} \otimes \mathbf{n} + \frac{\pi}{4}\omega \left(\mathbf{I} - \mathbf{n} \otimes \mathbf{n}\right) \tag{5}$$

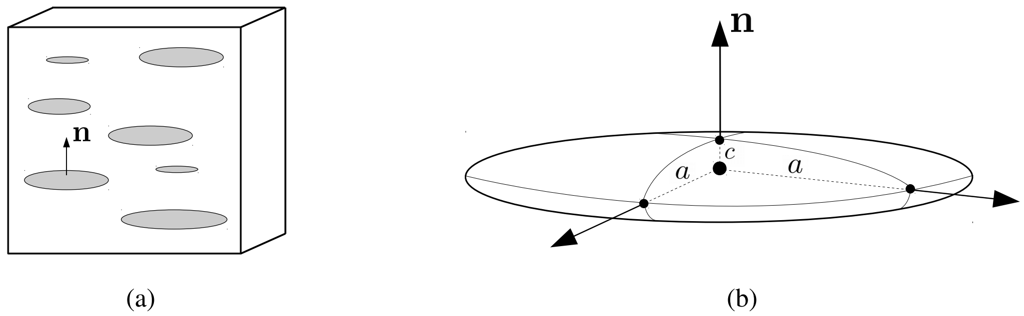

Figure 1: (a) RVE with single family of parallel microcracks, (b) penny-shaped crack geometry.

The configuration of the flat cracks corresponds to the limit case where $\omega \to 0$. This limit case has to be introduced at the very end of mathematical developments. As mentioned before, the unilateral effect is one of the main focus of this work. So, two different results can be obtained at the end, based on the state of the crack (open or closed). In either case, the cracks are assumed to be isotropic $\boldsymbol{\lambda}_c = \lambda_c \, \mathbf{I}$ (λ_c is the crack's scalar thermal conductivity) with different value of λ_c depending on the state of the crack:

- When the cracks are open, $\lambda_c = 0$, which supports the adiabatic conditions on the crack lips,
- When the cracks are closed, $\lambda_c = \lambda^*$, which accounts for some level of heat transfer continuity; this assumption is inspired by the works of Deudé *et al.* [5], where closed cracks are represented by a fictitious isotropic material with scalar conductivity $\lambda^* \neq 0$.

3 Calculation of the effective thermal conductivity

We impose a uniform macroscopic thermal gradient G at the outer boundary $\delta\Omega$ of the RVE. This is similar to the classical strain-based formulation in elasticity. As a first, we will estimate the effective conductivity through two different schemes. When there is a **dilute** concentration of cracks, it is considered there is no interaction between them. The remote condition in this case can be given by $G_\infty = G$. Hence, the localization tensor can be given by:

$$\langle \mathbf{A} \rangle_c^{dil} = \left[\mathbf{I} - \mathbf{S}_E \left(1 - \xi\right)\right]^{-1} \quad \text{with} \quad \xi = \frac{\lambda_c}{\lambda_m} \tag{6}$$

Now (4) can be written as

$$\boldsymbol{\lambda}_{hom}^{dil} = \lambda_m \left[\mathbf{I} - \frac{4}{3}\,\pi\, d\, \big(1-\xi\big)\,\mathbf{T}\right] \quad \text{with } \mathbf{T} = \lim_{\omega\to 0} \omega\, \Big[\mathbf{I} - \mathbf{S}_E\, \big(1-\xi\big)\Big]^{-1} \tag{7}$$

For open cracks, one has λ_c = 0, so $\xi = 0$, whereas $\lambda_c = \lambda^* \neq 0$ i.e. $\xi \neq 0$ for closed crack. Taking this into account, the expression for the effective conductivity tensor of the microcracked media is:

$$\boldsymbol{\lambda}_{hom}^{dil} = \begin{cases} \lambda_m \left[\mathbf{I} - \dfrac{8}{3}\, d\, (\mathbf{n}\otimes\mathbf{n})\right] & \text{if cracks are open} \\ \lambda_m\, \mathbf{I} & \text{if cracks are closed} \end{cases} \tag{8}$$

When we are to consider some interactions between cracks, the **Mori-Tanaka** scheme is used. The remote condition here is given by $G_\infty = \langle g\rangle_m$. Here the localization tensor is:

$$\langle \mathbf{A}\rangle_c^{MT} = \langle \mathbf{A}\rangle_c^{dil}\cdot \Big[(1-f_c)\,\mathbf{I} + f_c\,\langle\mathbf{A}\rangle_c^{dil}\Big]^{-1} = \Big[\mathbf{I} - \mathbf{S}_E\,(1-f_c)\big(1-\xi\big)\Big]^{-1} \tag{9}$$

This leads to:

$$\boldsymbol{\lambda}_{hom}^{MT} = \lambda_m \left(\mathbf{I} + \frac{4}{3}\,\pi\, d\,\mathbf{T}\right)^{-1} \tag{10}$$

As before, the specific behaviour of cracks according to their status gives the following:

$$\boldsymbol{\lambda}_{hom}^{MT} = \begin{cases} \lambda_m \left[\mathbf{I} - \dfrac{1}{1+\frac{3}{8d}}\,(\mathbf{n}\otimes\mathbf{n})\right] & \text{if cracks are open} \\ \lambda_m\, \mathbf{I} & \text{if cracks are closed} \end{cases} \tag{11}$$

Detailed developments can be found in [12].

4 Numerical simulations

In the following, numerical simulations are performed using Finite-Element software Abaqus®. $(\mathbf{X},\mathbf{Y},\mathbf{Z})$ denotes an orthonormal coordinate system. The simulated volume V is a cube (size $L = 1\ m$) that follows the steady state heat conduction. The matrix is designed as an unit 3D solid with its own scalar conductivity λ_m. Assuming there is only one crack in the volume, the radius of the crack can be given by $a = \sqrt[3]{d}$. It is logical to represent the crack as a seam for the open state (discontinuous nodes). Yet, it cannot account for the heat transfer during crack closure. So, the crack is modelled as an ellipsoidal inclusion (3D solid as well) with normal $\mathbf{n}$ belonging to $(\mathbf{X},\mathbf{Y})$ plane and has the scalar conductivity λ_c. Note that such description is in line with the theoretical framework. Since creating a crack with zero aspect ratio is not possible, the cracks are designed with an aspect ratio $0 \neq \omega << 1$ (so $f_c << 1$). Thus, for a given f_c, the value of the scalar conductivity λ_c determines if the cracks are open $(\lambda_c = 0)$ or closed $(\lambda_c = \lambda^* \neq 0)$. This description of the unilateral effect is in agreement with the theoretical model in Section 2. The finite element type used for both the matrix and crack is quadratic tetrahedron DC3D10 (see Fig. 2-a) and the model has approximately 26500 elements

and 19000 nodes including 289 nodes on the outer surface (see Fig. 2-b).
Temperatures T_1 and T_2 $(T_1 > T_2)$ are applied on the opposite faces of the volume with outer normals $\pm\,\mathbf{X}$ (see Fig. 2-c) while a zero flux condition is imposed on the other 4 faces. Such boundary condition, namely temperature gradient $G = \frac{\Delta T}{L}$, creates a heat flux Q inside the simulated volume. On a global point of view, the 4 faces with zero flux acts as an adiabatic wall, allowing the heat flux Q to be mainly oriented along the $\mathbf{X}$ direction. Therefore, the effective conductivity of the microcracked media can be given by:

$$\boldsymbol{\lambda}_{hom} = \lambda_{hom}\left(\mathbf{X}\otimes\mathbf{X}\right) \qquad \text{with} \qquad \lambda_{hom} = \left|\frac{Q_{\mathbf{X}}}{G}\right| \tag{12}$$

where heat flux along the $\mathbf{X}$ direction $Q_{\mathbf{X}} = \dfrac{1}{A}\displaystyle\sum_{i=1}^{n} RFL_i$, A is cross-sectional area and RFL_i is the reaction flux at a node i on the face $(+\mathbf{X})$.

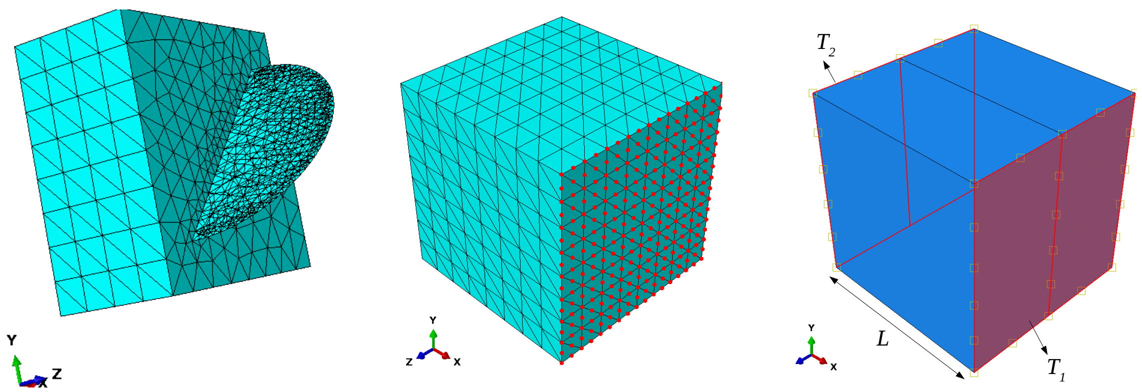

(a) (b) (c)

Figure 2: Simulated volume showing: (a) half the inclusion (half the volume hidden), (b) outer face nodes used for extracting results and (c) boundary condition.

As first illustration, Figure 3 shows the heat flux vector at integration points in a $(\mathbf{X}, \mathbf{Y})$ cutting plane for density $d = 0.1$. Figure 3-(a) corresponds to the open case $(\lambda_c = 0)$ and shows that the crack acts as a thermal barrier according to the adiabatic behaviour on their lips. Figure 3-(b) corresponds to the closed case $(\lambda_c = 50\%\ \lambda_m)$ and shows continuity in heat transfer. In both cases, we see that the heat flux vectors at the outer face with normal $-\mathbf{X}$ are not uniform. Hence, averaging in required. This is in accordance with the definition of the macroscopic quantities mentioned in Section 2.

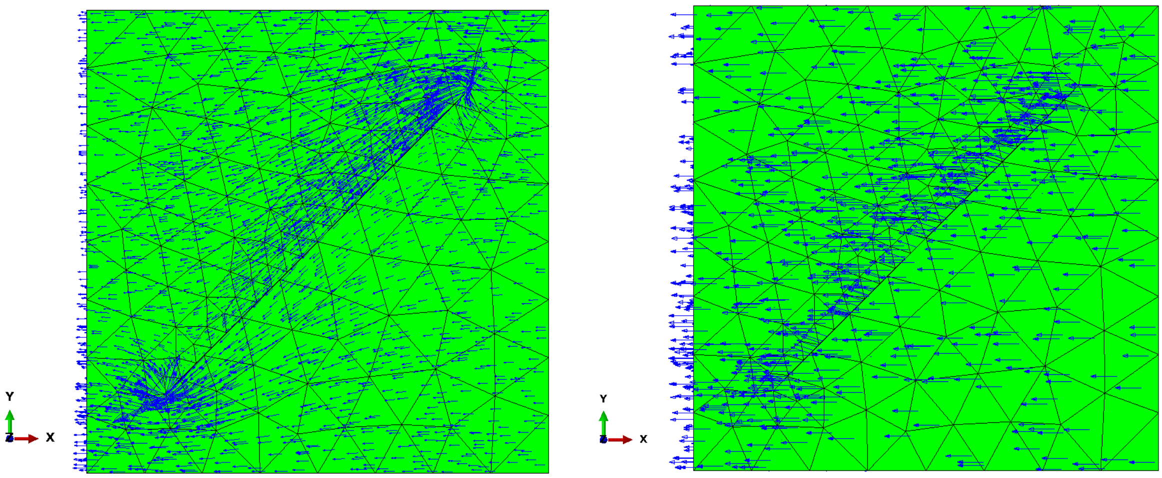

(a) Open crack (b) Closed crack

Figure 3: Heat flux vectors at integration points inside the simulated volume in a $(\mathbf{X}, \mathbf{Y})$ cutting plane.

5 Results and discussion

The general scalar conductivity $\lambda(\mathbf{v})$ in the direction of unit vector $\mathbf{v}$ can be given as $\lambda(\mathbf{v}) = \mathbf{v} \cdot \boldsymbol{\lambda}_{hom} \cdot \mathbf{v}$. Recalling our earlier results from [12], open cracks contribute to the degradation of the thermal conductivity, mainly along the direction $\mathbf{n}$ normal to the crack surface. This case is true for the simulations as well (see Fig. 4). Both the theoretical and simulated results show us damage induced anisotropy irrespective of the scheme or crack density. Regarding the theoretical models, we see that as $d \to 0$, $\boldsymbol{\lambda}^{dil}_{hom} \approx \boldsymbol{\lambda}^{MT}_{hom}$ ($d = 0.1$ in Fig. 4-a, $d = 0.02$ in Fig. 4-b). This can be attributed to the fact that as d decreases, the size of the crack decreases, making the interaction between the cracks less influential and at one point there is no interaction between the cracks essentially leading to a dilute configuration. We also see that as the crack becomes smaller, so does its influence on the conductivity ($\lambda(\mathbf{n}) \approx 0.75\ \lambda_m$ for $d = 0.1$ whereas $\lambda(\mathbf{n}) \approx 0.95\ \lambda_m$ for $d = 0.02$). Figure 4 also illustrates the consistency between the theoretical and simulated results. Even if only one crack is considered (no interaction case), the length scale separation assumed in theoretical approach is not applicable for the simulated volume V. That is why simulation curves do not exactly fit the dilute case.

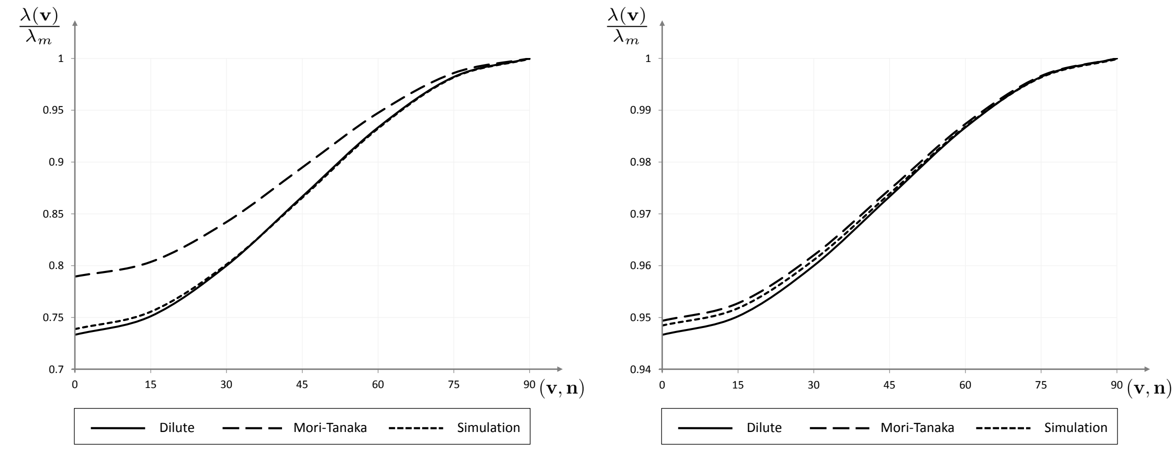

(a) $d = 0.1$ (b) $d = 0.02$

Figure 4: Generalized thermal conductivity $\lambda(\mathbf{v})$ normalized by its initial value for a material weakened by a single array of parallel open microcracks of unit normal $\mathbf{n}$.

On the other hand, dilute and Mori-Tanaka schemes show that closed cracks do not contribute to the degradation of conductivity (see (8) and (11)), i.e. the effective conductivity in any direction is recovered to its initial value at the crack closure. So the generalized scalar conductivity in unit direction $\mathbf{v}$ for closed cracks can be given as: $\lambda(\mathbf{v}) = \lambda_m, \ \forall \, \mathbf{v}$. Just like the open crack, simulated and theoretical results are consistent for the closed crack (see Fig. 5). We also see that the former has only a negligible amount of degradation of thermal conductivity (less than 0.05% for $d = 0.1$ and less than 0.01% for $d = 0.02$ when considering $\lambda^* = 50\% \ \lambda_m$).

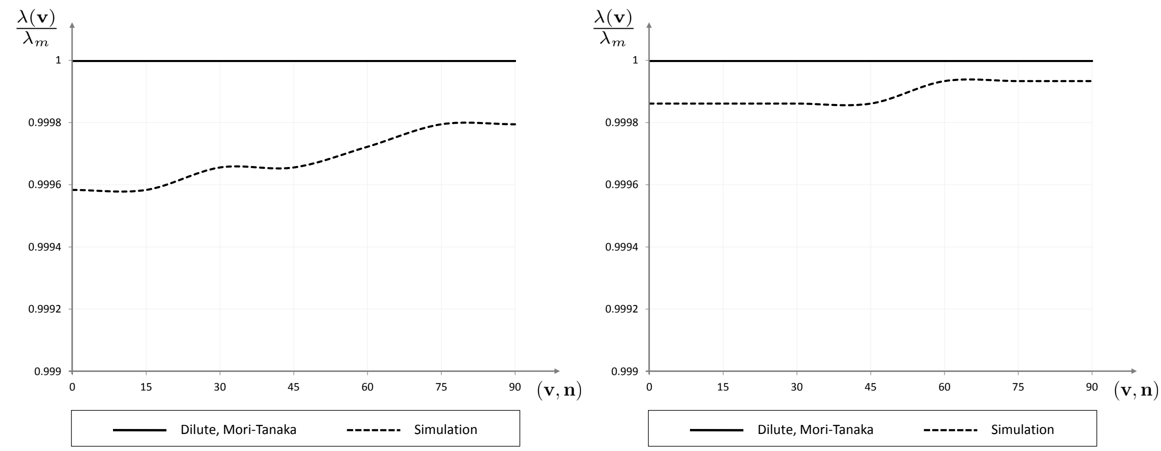

(a) $d = 0.1$ (b) $d = 0.02$

Figure 5: Generalized thermal conductivity $\lambda(\mathbf{v})$ normalized by its initial value for a material weakened by a single array of parallel closed microcracks of unit normal $\mathbf{n}$ $(\lambda^* = 50\% \ \lambda_m)$.

From (8) and (11) we know that the theoretical results are not a function of the aspect ratio ω $\left(\boldsymbol{\lambda}^{dil}_{hom} = \boldsymbol{\lambda}^{MT}_{hom} = f(\lambda_m, d, \mathbf{n})\right)$ since they correspond to the limit case $\omega \to 0$. But as discussed earlier, it is not possible to simulate an ellipsoid with zero aspect ratio. So it seems natural to study the influence of the aspect ratio on the simulated results. Since the maximum degradation is along the direction $\mathbf{n}$ normal to the crack, we intend to focus only on $\lambda(\mathbf{n})$. Figure 6-(a) corresponds to open crack and Figure 6-(b) corresponds to closed crack with fixed values of dilute and MT denoted for reference. In both cases, the variation in the results is very small (relative variation is around 0.5% and 0.4% respectively between extreme values of the aspect ratio). Yet, especially in the closed case, as $\omega \to 0$ simulations tend to the full recovery of $\lambda(\mathbf{n})$, same as the theoretical models. Note that all the simulations linked to varying aspect ratio are performed by varying the crack thickness c and keeping the crack density d and radius a as constant.

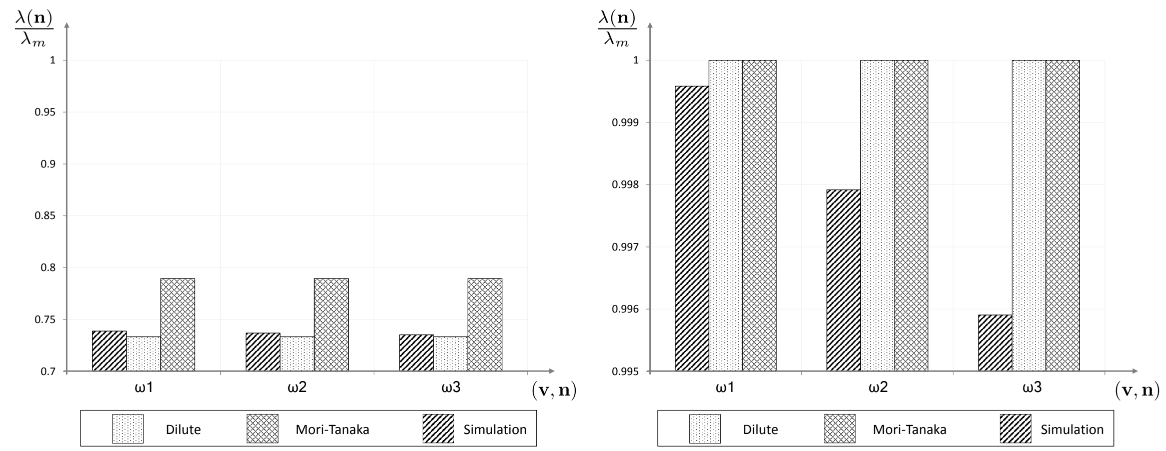

(a) Open cracks (b) Closed cracks

Figure 6: Normal thermal conductivity $\lambda(\mathbf{n})$ normalized by its initial value for various aspect ratios $\big(\omega 1 = 10^{-3}, \omega 2 = 5 \times 10^{-3}, \omega 3 = 10^{-2}; d = 0.1\big)$.

Also, the theoretical results for the closed case do not depend on the fictitious scalar conductivity λ^*. This may not be true for the simulations. So, series of simulations were performed with varying λ^* and for different aspect ratios (d and a are still constants). The values for λ^* are given as a proportion of λ_m such that $\lambda^* = \alpha\ \lambda_m$ with α = $\{1, 5, 10, 25, 50, 80, 100\}[\%]$. Figure 7 shows that indeed there is an influence of the scalar conductivity λ^* on the thermal conductivity. For $\alpha \leq 10\%$, we see drastic decrease in the conductivity, this is due to the fact that we are slowly approaching the open case ($\alpha = 0$). We also observe that as $\omega \to 0$ the influence of λ^* diminishes and representation of closed cracks by means of a 3D ellipsoid with fictitious scalar conductivity λ^* becomes independent of the λ^* value, just like the theoretical result [12].

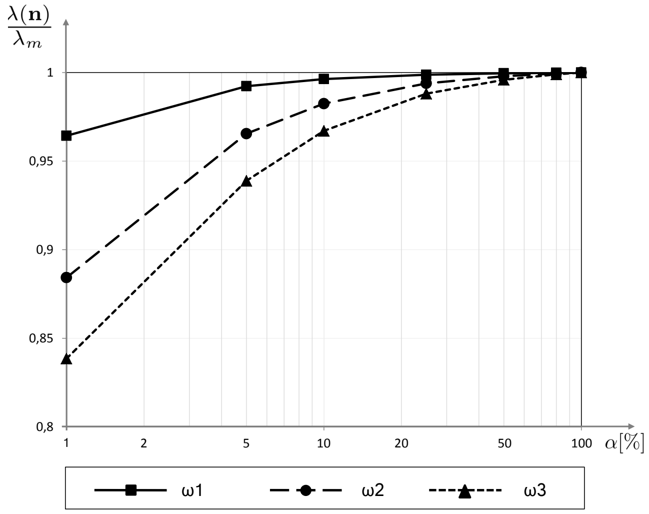

Figure 7: Influence of scalar conductivity λ^* on the normal thermal conductivity $\lambda(\mathbf{n})$ normalized by its initial value $\big(\omega 1 = 10^{-3}, \omega 2 = 5 \times 10^{-3}, \omega 3 = 10^{-2}; d = 0.1$; $\log$ scale is used for abscissa$\big)$.

6 Conclusion and perspectives

In this work, we have presented the closed-form expressions for the effective thermal conductivity of a microcracked media taking into account the steady state heat condition. Special attention has been paid to the unilateral effect and the consequence of the crack's state (open or closed) on the overall thermal behaviour. The consistency between numerical simulations and theoretical results validates some of the main assumptions of the study, especially regarding the geometric representation of cracks and the account of closed defect. Further studies could be conducted to extend such analytic procedure (homogenization and numerical simulations) to the case of flux-based boundary condition from which effective thermal resistivity can be derived.

References

[1] M. Kachanov, Advances in Applied Mechanics, vol. 30, Academic Press, New York, 1993.

[2] S. Nemat-Nasser, M. Hori, Micromechanics: Overall Properties of Heterogeneous Materials, In: Applied Mathematics and Mechanics, vol. 37, Elsevier Science, Amsterdam, 1993.

[3] I. Sevostianov, M. Kachanov, On the effective properties of polycrystals with intergranular cracks, Int. J. Solids Struct., 156–157 (2019) 243–250.

[4] X. D. Wang, L. Y. Jiang, The effective electroelastic property of piezoelectric media with parallel dielectric cracks, Int. J. Solids Struct., 40 (2003) 5287–5303.

[5] V. Deudé, L. Dormieux, D. Kondo, V. Pensée, Propriétés élastiques non linéaires d'un milieu mésofissuré, C. R. Mécanique, 330 (2002) 587–592.

[6] S. Torquato, Random Heterogeneous Materials. Microstructure and Macroscopic Properties, Springer Science+Business Media, New York, 2002.

[7] R. Hill, Elastic properties of reinforced solids : some theoretical principles, Int. J. Mech. Phys. Solids, 11 (1963) 357–372.

[8] J. D. Eshelby, The determination of the elastic field of an ellipsoidal inclusion, and related problems, Proc. R. Soc. A, 421 (1957) 379–396.

[9] J. G. Berryman, Generalization of Eshelby's formula for a single ellipsoidal elastic inclusion to poroelasticity and thermoelasticity, Phys. Rev. Lett., 79 (1997) 1142–1145.

[10] B. Budiansky and R. O'Connell, Elastic moduli of a cracked solid, Int. J. Solids Struct., 12 (1976) 81–97.

[11] H. Hatta, M. Taya, Equivalent inclusion method for steady state heat conduction in composites, Int. J. Eng. Sci., 24 (1986) 1159–1172.

[12] S. R. Rangasamy Mahendren, H. Welemane, O. Dalverny, A. Tongne, Thermal conduction properties of microcracked media: accounting for the unilateral effect, Submitted.